Polyethylene-carbon material for polymer electrolyte membrane fuel cell bipolar plates

P Greenwood*, **R Chen,** and **R H Thring**
Department of Aeronautical and Automotive Engineering, Loughborough University, Loughborough, UK

The manuscript was received on 22 August 2007 and was accepted after revision for publication on 26 February 2008.

DOI: 10.1243/14644207JMDA172

Abstract: Bipolar plates are the interconnects between cells within a fuel cell stack. They must be highly electrically conductive in order to maximize the voltage across the stack and must be highly thermally conductive to aid cooling of the stack. Traditionally, bipolar plates are made from graphite or stainless steel; both have drawbacks such as low mechanical strength and corrosion problems, respectively. In order to overcome the problems associated with these common materials and to improve on the electrical and thermal conductivity aspects as well as decrease costs and improve manufacturability, a mixture of polyethylene and carbon was investigated. Composites of polyethylene and carbon were mixed using a two-roll mill and injection moulded. Micrographs of the polyethylene-carbon (PE-C) blends show how the microstructure of the polyethylene network and carbon particles provide increased mechanical properties but further addition of carbon leads to the degradation of these properties. Increasing carbon content led to an ever-increasing electrical conductivity. The material was tested for tensile and flexural properties, resulting in a maximum tensile and flexural strength of ∼24 MPa (at 26 wt% carbon in polyethylene) and ∼35 MPa (at 40 wt% carbon in polyethylene), respectively. The samples displayed electrical conductivity, with a maximum of 1.19 S/cm in-plane and 1.05 S/cm through-plane being achieved at a carbon loading of 65 wt%. The PE-C composite displayed low densities of 1.56 g/cm^3 and desirable mechanical strength close to the US Department of Energy target level of 44.26 MPa for flexural strength. It was concluded that PE-C composites with different types of carbon and carbon fibres should be tested in order to reach the electrical conductivity target levels of 100 S/cm.

Keywords: fuel cells, bipolar plate

1 INTRODUCTION

Fuel cells have the potential to deliver clean electrical power from hydrogen and oxygen at high efficiencies of up to 60 per cent (80 per cent with combined heat and power systems). A lot of work has been done on membrane electrode assemblies (MEAs) and the catalyst layer, but research into bipolar plates is falling behind.

Bipolar plates connect one cell to another in series to build up the voltage within a stack and hence increase power output. They provide a way to distribute reactant gases to the reaction sites on the MEAs through channels cut out of the bipolar plate surface. They conduct heat away from the cells to control the stack-operating environment. They can be helpful in preventing water build-up within the stack by removing water droplets via the channels.

A two-cell stack is shown in Fig. 1 where the bipolar plate connects the two MEA active areas together. There are gaskets on either side of the membrane to seal the structure to prevent hydrogen escape. Two endplates similar to the bipolar plate are used to hold the structure together via bolts.

The requirements of a bipolar plate are as follows.

1. Provide high electrical conductivity to reduce electrical losses over the entire stack.
2. Supply and evenly distribute reactant gases over the active area of the cells to fully utilize all the reaction sites.

*Corresponding author: email: p.s.greenwood@lboro.ac.uk

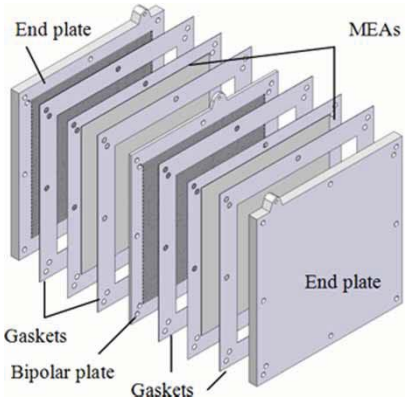

Fig. 1 Stack components of a two-cell stack showing two endplates sandwiching a bipolar plate between two MEAs and their gaskets

3. Remove water easily through the channels, mainly from the cathode side, to prevent flooding of the stack and hence deterioration in performance.
4. Withstand mechanical forces such as flexural and compression forces upon compaction of the stack.
5. Be low in cost to make them affordable and reduce the overall cost of the stack.
6. Easy to manufacture, i.e. for mass production, in order to help in reducing costs.
7. Provide high thermal conductivity to conduct heat away from the cells to prevent the cells drying out.
8. Must be impermeable to hydrogen and thus other gases to prevent cross-contamination of the gas streams.

To enable the wide-spread use of fuel cells, they have to be made more reliable at low cost, i.e. their price per kilowatt needs to be reduced. In order to achieve this, their physical size needs to be reduced whereas their power output needs to be increased. Therefore, it is beneficial to reduce the electrical resistance of the plates as well as their thickness as there can be in the region about 500 plates within a single stack and so any deficiencies are magnified. Also bipolar plates and end plates contribute a large proportion to the overall mass compared with any other component and so any reduction in mass will be advantageous to a vehicle's performance, if used for automotive applications.

So far, the main materials for bipolar plates have been graphite (bonded with phenolic resin) and metals (specifically 316L stainless steel). These two materials have been shown to be suitable in terms of conductivity, 300 S/cm [**1**] and 51 S/cm [**2**] for graphite and stainless steel, respectively. They have acceptable lifetimes of 6000 h [**3**] for stainless steel (limited by corrosion) and greater for graphite. Niobium–titanium–tungsten (Ni–Ti–W) and nickel–chromium (Ni–Cr) are relatively expensive [**4**] and do not offer sufficient benefit for their increase in cost and aluminium although cheap is not sufficiently corrosion resistant [**5**]. Coatings on metals have improved corrosion resistance, but have not eliminated it, and add cost to the final product [**6**].

In general, metals and graphite have advantages and disadvantages. Metals are easy to form into bipolar plates and are adequately conductive. But metallic plates have corrosion problems that can lead to poisoning/contamination of the MEA [**3**].

Graphite plates are highly conductive and corrosion resistant; but the plates can be large in mass due to a thicker plate requirement for sufficient strength, expensive, and difficult to manufacture and mass produce.

A bipolar plate material exhibiting the same or greater electrical properties of graphite with the manufacturability of metal would be ideal.

There are many patents on bipolar plates from Dupont, PlugPower, Schunk, and SGL Carbon (Eisenhuth) to name a few. Commercially available bipolar plate materials based on graphite from Schunk and Eisenhuth come close to the ideal mentioned above and have been used for comparison in this paper.

As an indication of the requirements for bipolar plates, the US Department of Energy (DOE) in 1999 set a flexural strength target of 44.26 MPa [**7**] and electrical conductivity target of 100 S/cm [**7**] for their bipolar plates. The choice of any potential bipolar plate material would mainly be governed by its mechanical properties so that it could survive the stresses within the stack.

Investigations into increasing conductivity in polymers will be conducted, as polymers can be formed more easily than metals but many have little or no conductivity. In addition, when using an injection-moulding manufacturing process, it would present extremely fast manufacturing times at low costs. However, a lot of work is required in order to obtain electrical conductivities equal to or better than that of metals.

Injection moulding was the targeted manufacturing process as components can be rapidly produced ($<$10 s [**8**]) and would in turn produce lower component costs due to mass production.

Polymers come in two forms: thermosetting and thermoplastic. Thermosetting plastic products are made by cross-linking polymer chains in a chemical reaction, and the formed part cannot be re-formed nor can be melted, whereas thermoplastic polymers are able to be formed and re-formed through heating. There are two types of thermoplastic polymer: amorphous and crystalline. Amorphous polymers usually have a low-chemical resistance and poor fatigue and wear resistance, and these include polymers such as polyvinylchloride and polystyrene. Crystalline polymers have a high-chemical resistance and better

fatigue and wear properties and include polymers such as polypropylene and polyester.

Polyethylene is a crystalline thermoplastic and was chosen because it is more common (and hence cheaper) than other plastics. Specifically, Exxon Mobil's HMA 018 high-density polyethylene (HDPE) was chosen as it is an injection-moulding grade and has a melting point (129 °C) [**9**] greater than a normal fuel cell operating temperatures. More importantly, it has a low density (0.954 g/cm^3) [**9**] and a high melt flowrate of 30 g/10 min (American Society for Testing and Materials (ASTM) D1238 – 2.16 kg) [**9**]; therefore, it will be low in viscosity and will easily fill a complicated injection-mould cavity quickly.

It is possible to improve the conductivity of polyethylene by mixing carbon (or graphite) with it. Carbon used for the study was the cheap and readily obtainable Cabot Monarch 800 grade with a density of 1.7–1.9 g/cm^3 [**10**], which is mainly used for pigmentation in a variety of applications such as paints and leather [**11**].

By mixing polyethylene with carbon powder, it is hoped that the best of both the materials would combine. The polymer component would enable easier manufacturability at low cost and would predominantly provide the structure of the bipolar plate. The carbon component would hopefully allow an electrically conductive path through the polymer.

The two-roll mill technique was chosen as the mixing method, as it involved far lower material wastage than compounding. Although ultimately more accurate, the compounding method involved an unacceptably high amount of material wastage to attain such accuracy.

Carbon was mixed with the polymer with varying weight percentages and so the highest achievable carbon loading was gained in the hope that the more carbon within the composite material, the higher the conductivity. The polyethylene-carbon (PE-C) mixture was injection moulded under high pressure to aid compaction of the carbon powder to increase conductivity through increased physical contact between carbon particles.

Injection-moulded test bars had their tensile, flexural, and electrical conductivity properties measured and compared with common bipolar plate materials, other polymeric filler materials from the literature, and commercially available materials.

2 METHODS

2.1 Two-roll mill

A two-roll mill churns molten polymer between two heated rollers, and the separation distance between the rollers can be used to form sheets of material

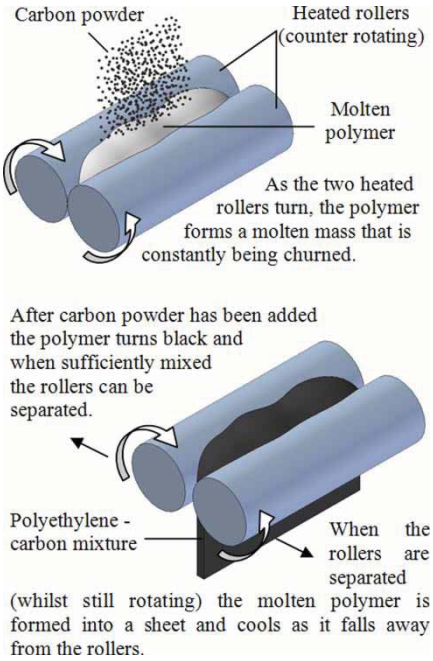

Fig. 2 Two-roll mill concept for mixing multiple components namely polymeric-based materials

(Fig. 2). As the material cannot be lost within the moving parts of the equipment, there is very little loss of material, and the process requires a fair amount of manual labour; therefore, the user can determine the level of homogeneity within the mixture.

Polymer was added to the two-roll mill heated to temperatures of 128 and 123 °C on the rear and front rollers, respectively. Once completely melted, carbon powder was added slowly and the two constituents were left to churn while a mill knife was used to spread the mixture around. The separation between the two-rollers was gradually widened and the resulting thick sheet was cut away from the front roller. The solidified composite sheet was then pelletized in a pelletizer. The process was repeated for 10, 20, 30, 40, 50, and 60 wt% carbon-loaded batches; five batches at each loading were produced, with each batch totalling 300 g.

2.2 Injection moulder

Injection moulders melt polymers through multiple heating stages and inject the melt into a cavity under high pressure. The mould cavity opens and the part is then ejected using pins that emerge from the face of the cavity. The process can be set up to run continuously with each injection + ejection cycle completing in less than a minute and hence large volumes of components can be manufactured within a short period of time, further reducing costs mainly due to the simplicity of the process.

The PE-C pellets were fed into the hopper where they were forced towards the nozzle by the rotation of

the screw. As they moved along the screw, the pellets were melted by the heating coils within the barrel to 180 °C. The screw moved back as more material was taken in (metering), and when the required volume (shot size) had been reached, the injection unit was ready for injection. The shot size for each test sample was 50 cm^3 and conformed to ASTM 638 Type I test bars. Each bipolar plate required a shot size of 88 cm^3, both the samples and plates were injected at pressures of 1500 bar.

Before injection, the two halves of the mould came together and the injection unit with its nozzle was pressed up against the heated sprue. During injection, the screw acted as a plunger and forced the molten material through the nozzle and sprue and into the mould under high pressure. Afterwards, the injection unit retracted, the two halves of the mould opened, and the ejector pins located on the movable half of the mould helped to free the part from the mechanism.

The test samples were formed via a channel in the mould directing the shot flow from the centrally placed sprue into the top of the test sample cavity. The longest length of the cavity was orientated along the vertical axis, producing a flow direction parallel to the length of the test sample. Only one test sample was created per shot cycle and the part of the solidified shot formed by the channel was sufficiently thin to be snapped off after ejection from the mould.

The bipolar plates were formed by direct injection into the centre of the mould cavity, as shown in Fig. 3. Owing to the complexity of the mould, the flow orientates itself around obstacles such as channel imprints and the bolt hole imprints within the cavity.

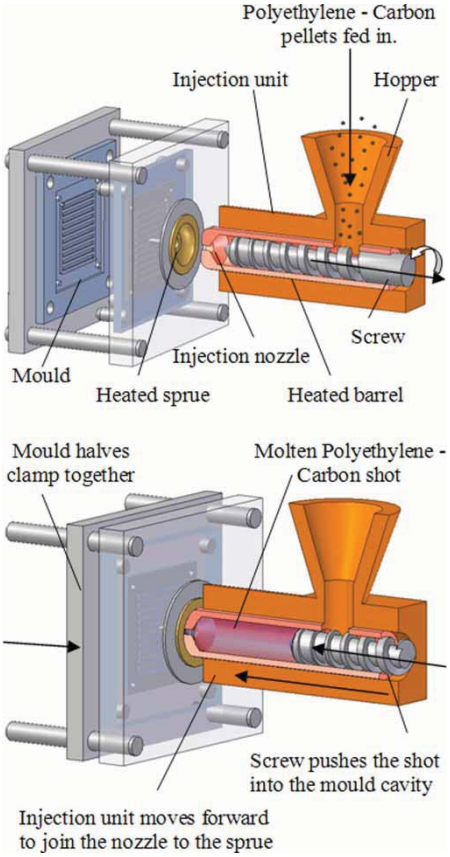

Fig. 3 Injection-moulding process (simplified) showing the metering and injection stages

3 TESTS

3.1 Ashing

Figure 4 shows the ashing test procedure used to determine the carbon contents of each batch of PE-C in weight per cent (wt%).

An empty crucible was weighed and the same crucible with a small amount of PE-C pellets was weighed again. It was then placed in an oven and after burning out the polymer at 400 °C for 10 min (including the ramping to and from 400 °C), the crucible containing plain carbon was weighed again. From the difference in masses of the PE-C and plain carbon after having subtracted the empty crucible mass, the percentage of carbon was calculated.

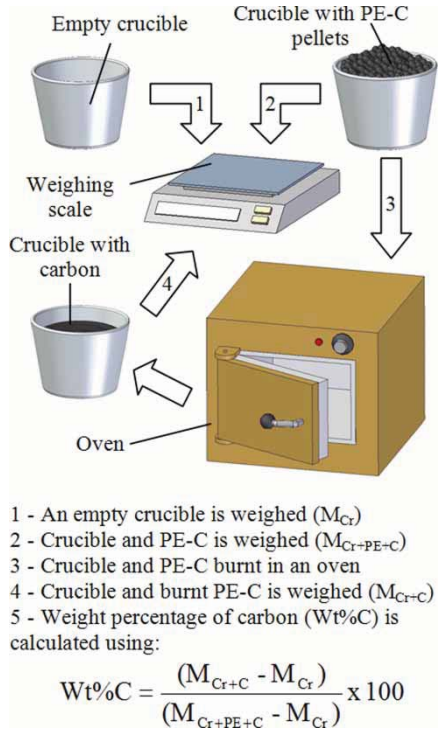

Fig. 4 Ashing test procedure used to determine the weight percentage of carbon for each PE-C batch

3.2 Tensile and flexural

A tensile test machine was used to pull the test specimens apart under a constant preset velocity. When fitted with a three-point bending apparatus,

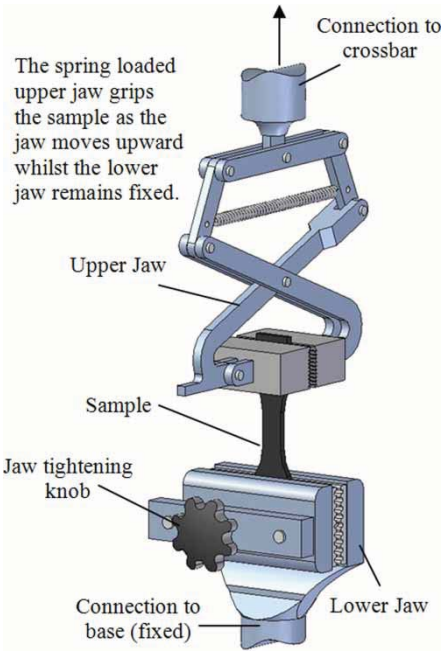

Fig. 5 Tensile test jaw set up for the tensile strength tests conducted with a 10 kN load cell

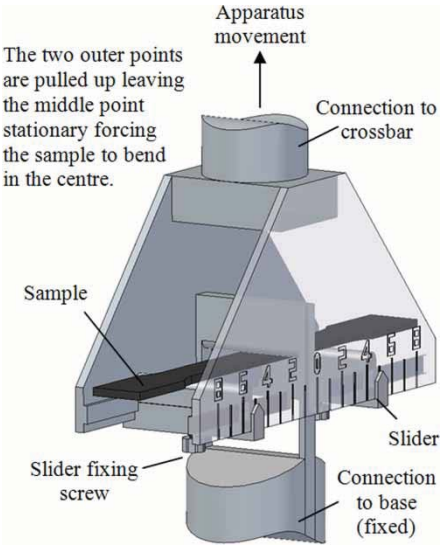

Fig. 6 Three-point bend test apparatus used for the flexural strength tests used with a 10 kN load cell

the machine will bend test samples under a constant velocity. Figures 5 and 6 show the test setup.

Each injection-moulded test sample was loaded into a tensile machine fitted with a 10 kN load cell. Five samples of each carbon loading were lined up along the central axis and clamped into the lower jaw and then clamped with the upper jaw. Any slack in the system was removed, the cross-head speed was set to 50 mm/min (ASTM D638) and the test was started; the results were recorded using a computer.

When fitted with the three-point bending apparatus, the mid-point of each sample was placed in line with the mid-point of the apparatus and any gap between the sample and the three contact points was zeroed. The middle point would push the mid-point of the sample downwards while the two outer points would act as pivot points on the sample. The forces measured by the same 10 kN load cell were then logged on a computer.

The apparatus was set to a span of 50 mm, the cross-head speed set to 2 mm/min according to ASTM D790, and the width and thickness of each sample were measured in three different locations and then averaged. Five samples for each carbon content were measured, and the flexural stress was given by equation (1)

$$\sigma_{\mathrm{F}} = \frac{3PL}{2bh^2} \tag{1}$$

where σ_{F} is the flexural stress, P the maximum load, L the span length, b the sample width, and h the sample thickness.

3.3 Electrical conductivity

The electrical resistance of each sample was measured with a Danbridge DB501 four-point probe. As shown in Fig. 7, two probes supply a current through the sample and the other two probes measure the potential difference. The use of four probes eliminates the effects of contact resistance that would otherwise obscure readings in samples of very low conductivity.

Each sample was cut into a $20 \times 20\,\mathrm{mm}^2$ with a thickness of 3 mm. In-plane measurements in line with the injection-moulding flow direction and through-plane measurements perpendicular to the flow were

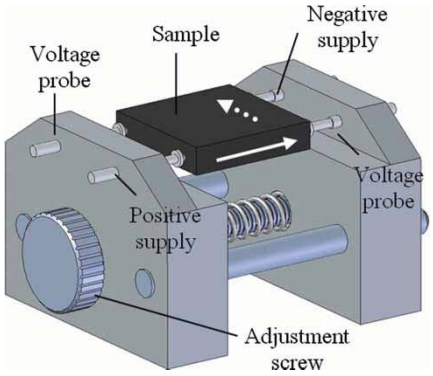

Fig. 7 Sample holder for electrical conductivity measurements. The four connections (positive supply, negative supply, and the two voltage probes) are connected to a Danbridge DB501 four-point probe. The white arrow indicates injection-moulding flow direction and the dotted white arrow indicates the perpendicular direction

obtained by placing two probes (1 mm needle probes) spaced 10 mm apart on each side of the sample. When changing samples, the contact pressures of the probes on each sample were made as equal as possible by using an adjustable stage. Then a resistance reading was noted from the readout on the display and converted to conductivity using equation (2)

$$\sigma = \frac{1}{\Omega \cdot A} \tag{2}$$

where σ is the conductivity (S/cm), Ω the resistance (ohms), and A the area of test sample (area cornered by the four test probes incorporating the sample thickness).

3.4 Field emission gun scanning electron microscope

The field emission gun scanning electron microscope (FEGSEM) shown in Fig. 8 differs from a normal SEM by using field emission to generate the electron beam instead of thermionic emission. It uses a finely tipped tungsten crystal; electrons are drawn from the filament tip by a potential field set up by the first anode below the tip of the filament. The electrons then travel down the column aided by the second anode. The electron beam passes through the first condenser lens where it is condensed, and coarse adjustments to the beam form and current can be made. The second condenser lens, where the fine control over the beam can be made, condenses the beam into a thin and tightly packed one. The beam is then made to scan in a grid-like fashion by the scanning coils to produce an image on a television monitor. The beam passes through the objective lens to be focused onto the desired part of the sample. The beam then hits the

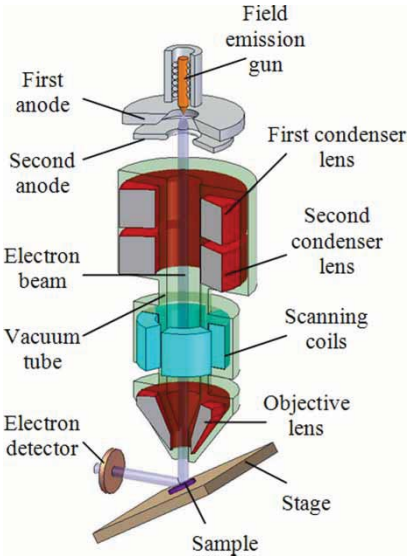

Fig. 8 Major components of FEGSEM

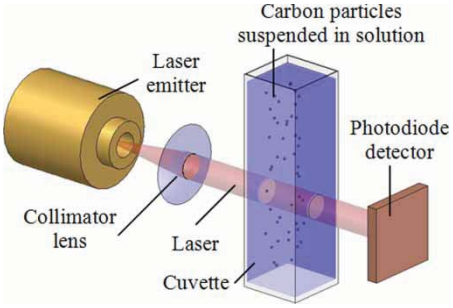

Fig. 9 Major components of the Malvern Zetasizer used to measure particle size

sample and any primary and/or secondary electrons are detected at the detector and then fed to the computer. The FEGSEM enables a narrower beam with spot sizes <2.0 nm, thus higher resolutions are obtained.

The samples were gold-coated and placed on the sample stage in a vacuum environment. A beam energy of 5 kV was used at 750 000× magnification.

3.5 Malvern Zetasizer

The Malvern Zetasizer (Fig. 9) measures particle sizes in the nanometre range. Particles of less than a few microns are measured by observing the Doppler shift of the incident light due to the Brownian motion of the suspended particles. Light will be scattered from the particles and its frequency will be shifted. The speed of the particles determines how much the frequency is shifted. By knowing the incident light frequency and measuring the scattered light frequency to determine the shift, the particle size can be calculated.

Carbon (1.5 mg) was placed in a glass sample tube with 30 ml of de-ionized water and two drops of Coulter laboratory reagent. The sample tube was shaken and then placed in an ultrasonic bath for 1 h. The mixture of carbon and water was further diluted by putting 3.5 ml of de-ionized water in a 4 ml cuvette along with six drops (0.375 ml) of the carbon–water mixture from a pipette. The cuvette was then shaken and placed in the Zetasizer. The Zetasizer was set to take an average particle size from 10 runs. This process was repeated twice more with a fresh cuvette filled with the same solution from the sample tube. The computer recording the readings then produced a plot of the particle size distribution.

4 RESULTS

4.1 Tensile and flexural

The results in Fig. 10 show the ultimate tensile strength of the samples with varying carbon content. There was a sharp increase in strength with increasing carbon content from ∼11 MPa at 0 wt%

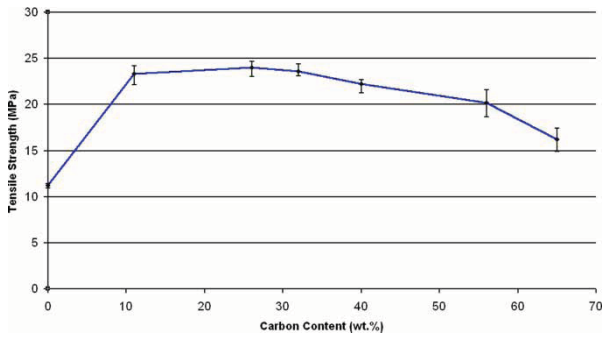

Fig. 10 Tensile test results of PE-C with increasing carbon content

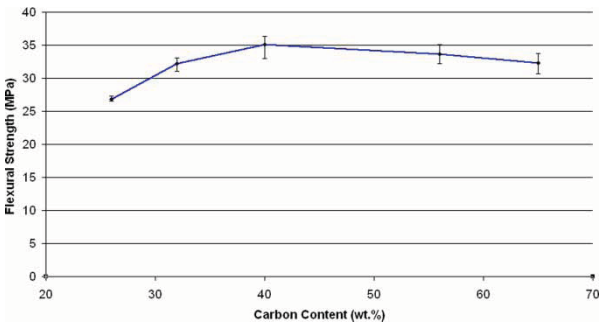

Fig. 11 Flexural stress results for increasing carbon content in a PE-C composite

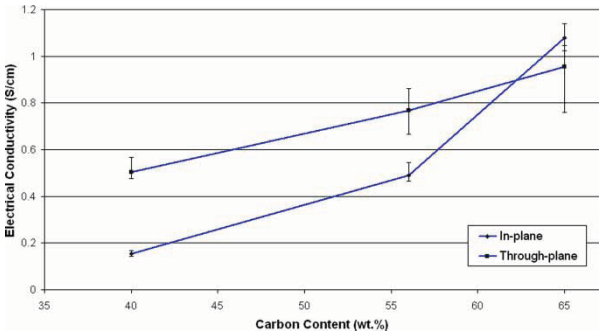

Fig. 12 In-plane and through-plane electrical conductivities of PE-C composite with increasing carbon content

to an optimum strength of ∼24 MPa at 26 wt%. Up to this point the increase in strength could be attributed to the composites ability to reduce fracture energy and crack propagation via the delamination of the carbon–polyethylene interfaces. Therefore the increase in carbon–polyethylene interfaces with the increase in carbon content would provide a greater potential for delamination. By further increasing the carbon content, the strength decreased gradually to ∼17MPa at 65 wt% and the samples fractured with increasing brittleness. The reason for increasing brittleness and decreasing strength was the increasing amounts of carbon–carbon interfaces and the decreasing amounts of carbon–polyethylene interfaces. Therefore, there would have been less delamination between the carbon–polyethylene interfaces and more routes for crack propagation between the carbon–carbon interfaces.

The low tensile strength of ∼11 MPa for the pure polymer was half the manufacturer's value of 22 MPa [**9**]. The test rate used in both cases was identical, 50 mm/min, using similar testing standards ASTM638 and ISO572 [**9**]. The difference could be attributed, in a small way, to the differences between the thickness of the samples used for ASTM638 and ISO572 where their dimensions differ, $12.5 \times 3.2\,\text{mm}^2$ and $10 \times 4\,\text{mm}^2$, respectively, but their cross-sectional areas are identical. Mostly, the difference could be attributed to the processing of the material i.e. the manufacturer's injection-moulding parameters may have differed from the parameters detailed in section 2.

Figure 11 shows the results of the flexural tests. It shows that there was a peak at 40 wt% where the maximum flexural strength was ∼35 MPa. Before the maximum, flexural strength increased rapidly but after the maximum, it decreased gradually. Samples with carbon content <26 wt% did not fracture.

The large rise in flexural strength up to the maximum was due to the lower carbon-loaded samples deforming plastically, and any increase in carbon content improved their stiffness adding to their strength. After the maximum, any addition in carbon content increased the samples' brittleness and so flexural strength remained high but gradually decreased, the cause of which are the carbon–carbon and carbon–polyethylene interfaces as mentioned previously.

The micrographs of the PE-C samples prove this theory. The polyethylene networks become increasingly thinner with increasing carbon content and so are less able to hold the overall structure together and larger and larger potential fracture paths are set up by the carbon–carbon interfaces.

The addition of carbon improved both the polyethylene's tensile and flexural strength properties. The tensile and flexural strengths of all the samples were higher than the original polyethylene, although the optimum carbon content for the tensile strength (26 wt%) did not match the optimum content for the flexural strength (40 wt%). For fuel cell use, bipolar plates are not subjected to tensile forces but are subjected to flexural forces and so choosing the optimal carbon content of 40 wt% would be more advantageous.

4.2 Conductivity

Figure 12 shows the results of the in-plane and through-plane conductivity tests. With increasing carbon content, the in-plane conductivity increased exponentially, more precisely, the rate of increase

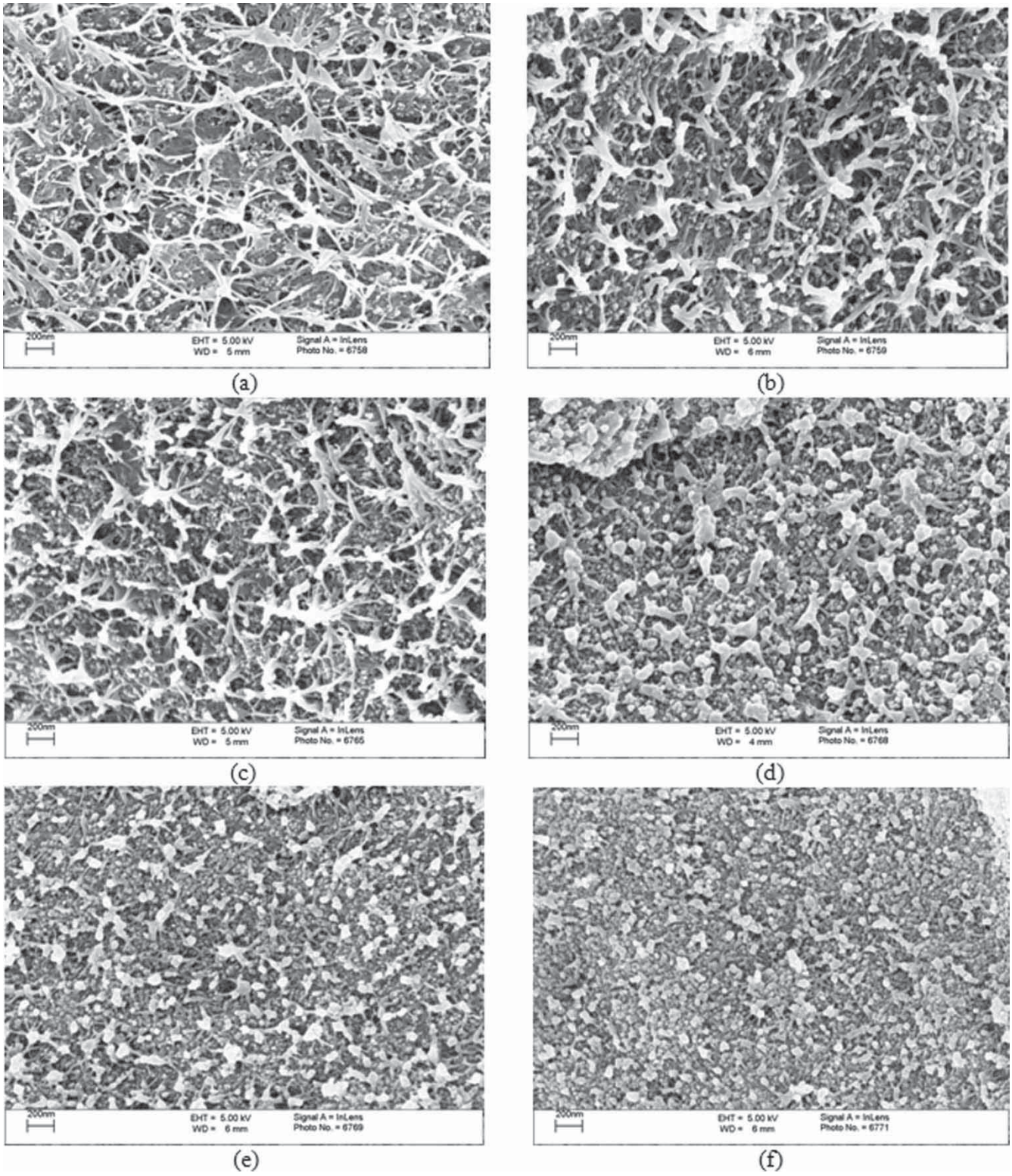

Fig. 13 FEGSEM micrographs of: (a) 11 wt%, (b) 26 wt%, (c) 32 wt%, (d) 40 wt%, (e) 56 wt%, and (f) 65 wt% of carbon in polyethylene

in conductivity from 56 to 65 wt% had more than tripled compared with 40–56 wt%. The through-plane conductivity increased fairly linearly, and although higher in conductivity at 40 and 56 wt% than the in-plane measurements, its value was less than the in-plane measurements at 65 wt%. Overall, samples below 40 wt% did not conduct at all. The in-plane minimum and maximum conductivities

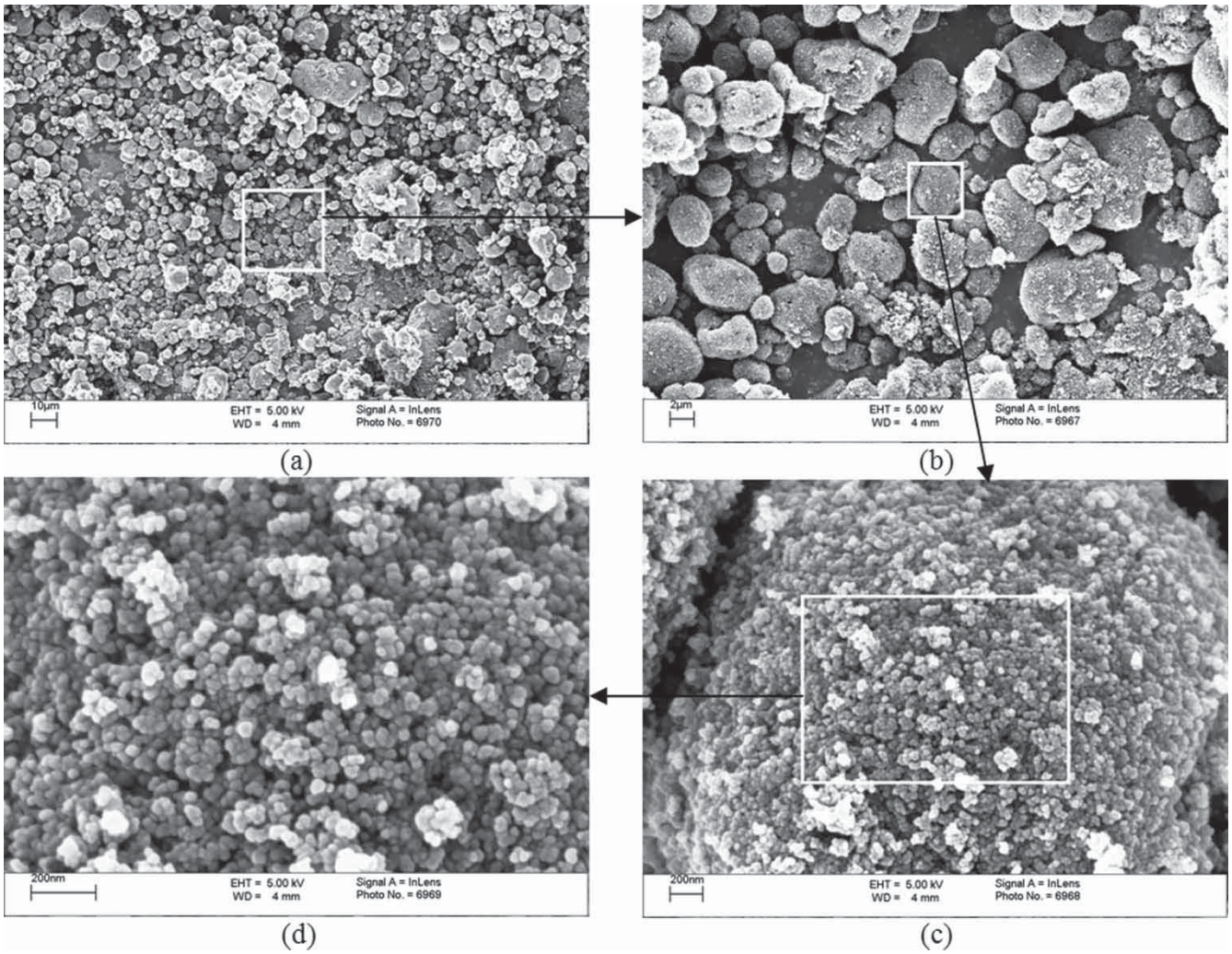

Fig. 14 Carbon powder FEGSEM micrographs showing primary structures (a) and (b), and secondary structures (c) and (d)

obtained were 0.16 and 1.19 S/cm, respectively, and the through-plane minimum and maximum conductivities obtained were 0.47 and 1.05 S/cm, respectively.

Even though the flexural strength of 40 wt% carbon material was ∼9 MPa less than the target strength of DOE (44.26 MPa), it probably would be good enough for stack use. However, at 40 wt%, the electrical conductivity was 0.16 S/cm in-plane and 0.47 S/cm through-plane. The results also revealed that with increasing carbon content, the more the conductivity varied within the same group, shown by the increasing error bar ranges for the points on the graph. To improve the conductive properties of the material as well as to produce replicable conductivities of samples within the same batch, carbon fibres of different lengths will be investigated using identical processing techniques to improve the contact surface area between the filler particles.

4.3 Microstructure

The micrographs in Fig. 13 are the fracture surfaces from 11 to 65 wt% carbon-loaded samples. They show a polyethylene network supporting small agglomerates of carbon powder. Each particle was on an average 38.46 nm in diameter. The 11 wt% sample, Fig. 13(a), showed a thick network of polyethylene with very few carbon particles. The polyethylene network becomes finer and the quantity of carbon particles increases as the carbon content increases. At 65 wt%, Fig. 13(f), there is a fine network of polyethylene with large amounts of carbon tightly packed and held together by the polyethylene network.

With increasing carbon content, there was a greater degree of contact between the carbon particles, hence the rapid increase in conductivity, but the extremely thin strands of the resulting polyethylene network were the cause of the material's brittleness.

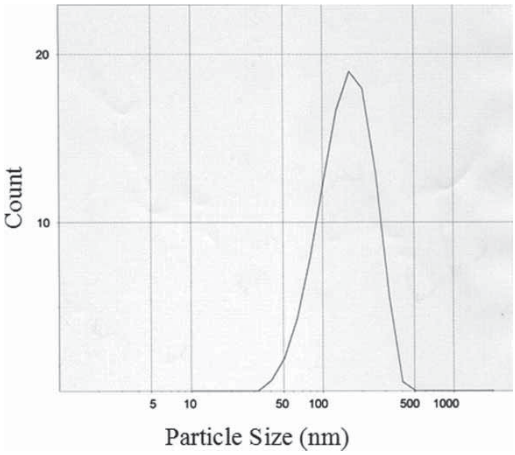

Fig. 15 Malvern-Zetasizer particle size test result with an average particle size of 149.05 nm

4.4 Particle size

The carbon powder in its unaltered form shows primary structures ranging from 2 to 25 μm in size (Figs 14(a) and (b)). These primary structures are made up of agglomerated carbon particles of 20 nm in size (Figs 14(c) and (d)).

Figure 15 shows the particle size plot taken from the powder, with the average particle size being 149.05 nm. This was more representative of small agglomerations (Fig. 14(d)) that were not broken up by ultrasonic action. It is possible that these small agglomerations were not broken up by the shear forces in the two-roll mill or the high pressure of the injection-moulding machine and may have remained in the final samples.

5 DISCUSSION

Table 1 shows that in comparison to other materials available for bipolar plates, the PE-C composite offers some advantages and disadvantages. The PE-C flexural strength was better than graphite and close to the commercially available materials from Schunk and Eisenhuth, but its conductivity was far from the existing conductivity values for bipolar plates, i.e. upto 300 S/cm [**2**] for graphite. This was mainly due to the Monarch 800 grade of carbon that was used for the investigation. This grade of carbon is not known for good electrical conductivity, only that it is used for pigmentation for various applications [**10**]. However, the conductivity was better than the other polymer-based material, CNT-PET/PVDF.

As the flexural strength of the material is a major factor, the ideal carbon content of 40 wt% gave the highest flexural strength but would only give a conductivity of 0.16 S/cm (Fig. 12) compared with the maximum achievable 1.19 S/cm. The highest flexural strength of ∼35 MPa was roughly five times higher than that of graphite and close to the DOE's target of 44.24 MPa.

The tensile result of ∼24 MPa was the lowest in the table; however, as bipolar plates are subjected to very little or no tensile forces in the stack environment, the magnitude of the result is not sufficient to put the material at a disadvantage. The density of the PE-C composite was the lowest in table. It was close to that of graphite but still requires improvement.

The commercially available materials based on graphite [**16**, **17**] had high conductivities and flexural strengths but had the penalty of higher densities i.e. $\geqslant 1.85\,g/cm^3$. The filler content in the Schunk plates is in the range of 70–95 wt% and formed by compression moulding [**16**]. The Eisenhuth grades (PPG, polypropylene; BMA, PVDF (up to 80 wt% [**17**]); and BBP, phenolic resin) were suitable for compression and injection moulding, except for the BMA 5 grade which was only suitable for compression moulding [**15**]. Both the material manufacturers have a high filler content resulting in the higher densities reported and thus

Table 1 Comparison of PE-C composite results with 316L stainless steel, aluminium, graphite, carbon nanotube-polyethylene terephalate/poly vinylidene difluoride (CNT-PET/PVDF), and commercially available bipolar plate materials from Schunk and Eisenhuth

Material	Electrical conductivity (S/cm)	Flexural strength (MPa)	Corrosion current/rate	Tensile strength (MPa)	Density (g/cm^3)
316L stainless steel	51 [**1**]	—	384 $\mu A/cm^{-2}$ (H_2)/586 $\mu A/cm^{-2}$ (air) [**4**] < 100 μm per year [**2**]	485 [**12**]	8.0 [**12**]
Al	—	—	∼250 μm per year [**2**]	90 [**12**]	2.7 [**12**]
Graphite	300 [**2**]	6.9 [**12**]	—	—	1.63 [**12**]
CNT-PET/PVDF	0.059 [**13**]	—	—	34 [**13**]	—
PE-C	1.19[a]/1.05[b]	∼ 35	—	∼ 24	1.56
Schunk FU4413	90.9[a]/35.7[b] [**14**][c]	50 [**14**]	—	—	1.88 [**14**]
Schunk FU4369	111[a]/52.6[b] [**14**][c]	40 [**14**]	—	—	1.9 [**14**]
Eisenhuth PPG 86	55.6[a]/18.2[b] [**15**][c]	40 [**15**]	—	—	1.85 [**15**]
Eisenhuth BMA 5	100[a]/20[b] [**15**][c]	40 [**15**]	—	—	2.1 [**15**]
Eisenhuth BBP 4	200[a]/41.7[b] [**15**][c]	40 [**15**]	—	—	1.97 [**15**]

[a]In-plane conductivity; [b]through-plane conductivity; [c]conductivity converted from resistivity.

would increase stack weight and bipolar plate costs due to filler costs.

There were large variations between the in-plane and through-plane conductivities of the Schunk and Eisenhuth materials. The through-plane conductivities were 53–80 per cent less than the in-plane conductivities compared with the 12 per cent decrease of the PE-C material, although this value may increase if the trend from Fig. 12 continues beyond the 65 wt% loading.

In order to improve the conductivity, different forms of graphite and/or carbon will be tried and possibilities include spherical graphite particles, graphite filaments, and carbon fibres of various lengths.

A highly (more expensive) conducting powder such as Vulcan XC-72 in its dry powder state is capable of producing conductivities of ∼7.4 S/cm [**18**]. After processing, this value would be much higher due to the high compaction forces in injection and compression moulding.

There is also a need for achieving better electrical contacts between the adjacent carbon particles. Ways of addressing this issue will be investigated with a view to increasing contact surface area via different filler shapes and orientation, for example, in the case of fibre fillers.

Compression moulding will be looked at as another cheap and fast production process. An alternative mixing technique will be investigated to ensure that ideal, not approximate, mixtures are obtained.

Further tests to fully investigate the material's behaviour within a fuel cell environment will be conducted. These include thermal conductivity to predict heat dissipation, hydrogen permeability, and material stability. More tests such as fracture toughness would give a better understanding of the material's behaviour when compared with the tensile and flexural strength results.

6 CONCLUSIONS

1. The ashing tests showed that the actual carbon contents varied from the intended contents by as much as 6 per cent. Therefore, the two-roll mill process is not the ideal equipment to use if exact mixtures are required.
2. As the carbon content increased, so did the tensile and flexural strengths. The optimums for the tensile and flexural strengths were at 26 wt% (∼24 MPa) and 40 wt% (∼35 MPa), respectively, the latter being somewhat lower than the DOE target of 44.26 MPa.
3. Beyond the optimums, the quantity of carbon particles within the composite starts to have an effect on the material's ability to form a thick network of polyethylene to help bind carbon together. As the polyethylene network becomes sparse, the material's strength reduces.
4. With the addition of carbon up to 65 wt%, even with the degradation of properties beyond the optimums, both the flexural and tensile results exhibited higher values than the 100 per cent polyethylene samples.
5. There is a trade-off between strength and conductivity but for fuel cell use, the selection of material is likely to hinge more on its mechanical properties provided that its conductivity is sufficient enough (e.g. $\geqslant$100 S/cm [**7**]).
6. The conductivity at maximum flexural strength (at 40 wt%) was 0.16 S/cm measured in-plane and 0.47 S/cm through-plane. With increasing conductivity, the results become more dispersed, but the material exhibited more dimensional stability between the in-plane and through-plane conductivities compared with the commercially available materials. The maximum conductivities achieved were 1.19 S/cm in-plane and 1.05 S/cm through-plane.
7. The conductivity gained from the PE-C samples was insufficient as an ideal bipolar plate material, but the results showed the feasibility of mixing polymers with carbon fillers for further development and the potential for other fillers such as carbon fibre intended for the next stage of the investigation.

REFERENCES

1 **Wind, J., Spah, R., Kaiser, W.,** and **Bohm, G.** Metallic bipolar plates for PEM fuel cells. In 7th Ulmer Elektrochemische Tage, 26–27 June 2000, pp. 256–260 (Elsevier Science B.V., Amsterdam).

2 **Lee, S., Huang, C.,** and **Chen, Y.** Investigation of PVD coating on corrosion resistance of metallic bipolar plates in PEM fuel cell. *J. Mater. Process. Technol.,* **140**(1–3) (special issue), 688–693.

3 **Makkus, R. C., Janssen, A. H. H., De Bruijn, F. A.,** and **Mallant, R. K. A. M.** Use of stainless steel for cost-competitive bipolar plates in SPFC. *J. Power Sources*, **86**, 274–282.

4 **Brady, M. P., Weisbrod, K., Zawodzinski, C., Paulauskas, I., Buchanan, R. A.,** and **Walker, L. R.** Assessment of thermal nitridation to protect metal bipolar plates in polymer electrolyte membrane fuel cells. *Electrochem. Solid-State Lett.,* 2002, **5**(11), 245–247.

5 **El-Khatib, K. M., Abou Helal, M. O., El-Moneim, A. A.,** and **Tawfik, H.** Corrosion stability of SUS316L HVOF sprayed coatings as lightweight bipolar plate materials in PEM fuel cells. *Anti-Corros. Methods Mater.,* 2004, **51**(2), 136–142.

6 **Cunningham, N., Guay, D., Dodelet, J. P., Meng, Y., Hlil, A. R.,** and **Hay, A. S.** New materials and procedures to protect metallic PEM fuel cell bipolar plates. *J. Electrochem. Soc.,* 2002, **149**(7), 905–911.

7 **Cooper, J. S.** Design analysis of PEMFC bipolar plates considering stack manufacturing and environment impact. *J. Power Sources*, 2004, **129**, 152–169.

8 **Middelman, E., Kout, W., Vogelaar, B., Lenssen, J.,** and **De Waal, E.** Bipolar plates for PEM fuel cells. In Proceedings of Scientific Advances in Fuel Cell Systems, 25–26 September 2002, pp. 44–46 (Elsevier Science B.V., Amsterdam).

9 *ExxonMobil HDPE HMA018 Datasheet*, ExxonMobil 2003, available from www.exxonmobilpe.com/Public_Files/ Polyethylene/Polyethylene/Europe/Data_Sheet_ExxonMobil_HDPE_HMA_018.pdf

10 *Cabot Monarch 800 Materials Safety Data Sheet*, 2005. Cabot Corporation, available from http://www.cabot-corp.com/ cws/product.nsf/PDSDOCKEY/∼∼∼M800

11 *Cabot Materials Data Sheet*, 2002. Cabot Corporation, available from http://www.cabot-corp.com/cws/product.nsf/PDSDOCKEY/∼∼∼M800

12 **Carvill, J.** *Mechanical engineers data handbook*, 1999 (Butterworth-Heinemann, Oxford).

13 **Man, W.** and **Leon, L. S.** On the improved properties of injection-molded, carbon nanotube-filled PET/PVDF blends. *J. Power Sources*, 2004, **136**, 37–44.

14 *Schunk Moulded Bipolar Plate Datasheet*, Schunk Kohlenstofftechnik GmbH, available from http://www.schunk-fuelcells.com/sixcms/media.php/1722/08_02e.pdf

15 *Eisenhuth Sigracet Bipolar Plate Datasheet*, Eisenhuth, available from http://www.eisenhuth.de/pdf/SIGRACET_Datenblaetter.pdf

16 Schunk Kohlenstofftechnik GmbH, *Bipolar plate press device and method for production thereof*. World Intellectual Property Organisation Pat. WO03047016, 2003.

17 SGL Carbon AG, *Bipolar plate for fuel cell stacks*. US Pat. 6706437, 2004.

18 **Pantea, D., Darmstadt, H., Kaliaguine, S., Sümmchen, L.,** and **Roy, C.** Electrical conductivity of thermal carbon blacks: influence of surface chemistry. *Carbon*, 2001, **39**, 1147–1158.

APPENDIX

Notation

A	area of test sample
b	sample width
h	sample thickness
L	span length
M_{Cr}	empty crucible mass
$M_{\mathrm{Cr+C}}$	mass of crucible + carbon
$M_{\mathrm{Cr+PE+C}}$	mass of crucible + polyethylene + carbon
P	maximum load
wt%	percentage of carbon by weight
σ	conductivity (S/cm)
σ_{F}	flexural stress
Ω	resistance (ohms)